**Electronic Supporting Information**

# Photophysics and Charge Transfer in Oligo(thiophene) Based Conjugated Diblock Oligomers

Habtom B. Gobeze, Pradeepkumar Jagadesan, and Kirk S Schanze*

University of Texas at San Antonio, Department of Chemistry, One UTSA Circle, San Antonio, TX 78249.

* Corresponding author email: kirk.schanze@utsa.edu

## Synthesis and Characterization

Precursors **T4**[1], **T4-SnBu$_3$**[2], **TBT-Br**[3], **T4-Br**[4], **T8**[5], **T8-Br**[6], **TBT-SnBu$_3$**[7] were synthesized by following reported procedure.

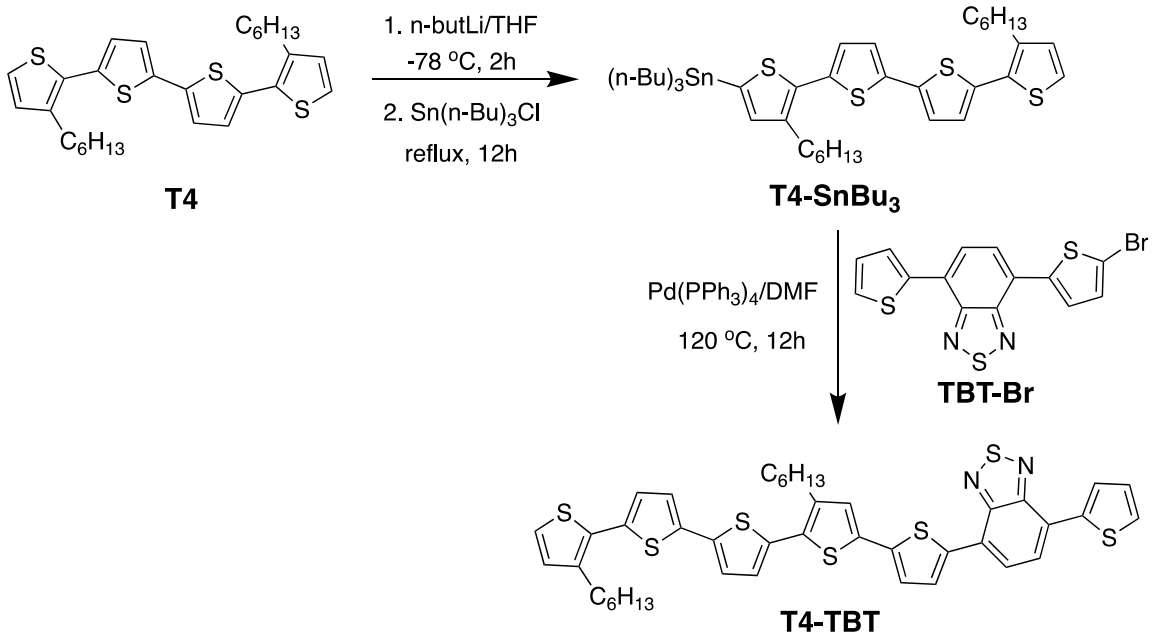


**Scheme S1.** Synthesis of **T4-TBT**.

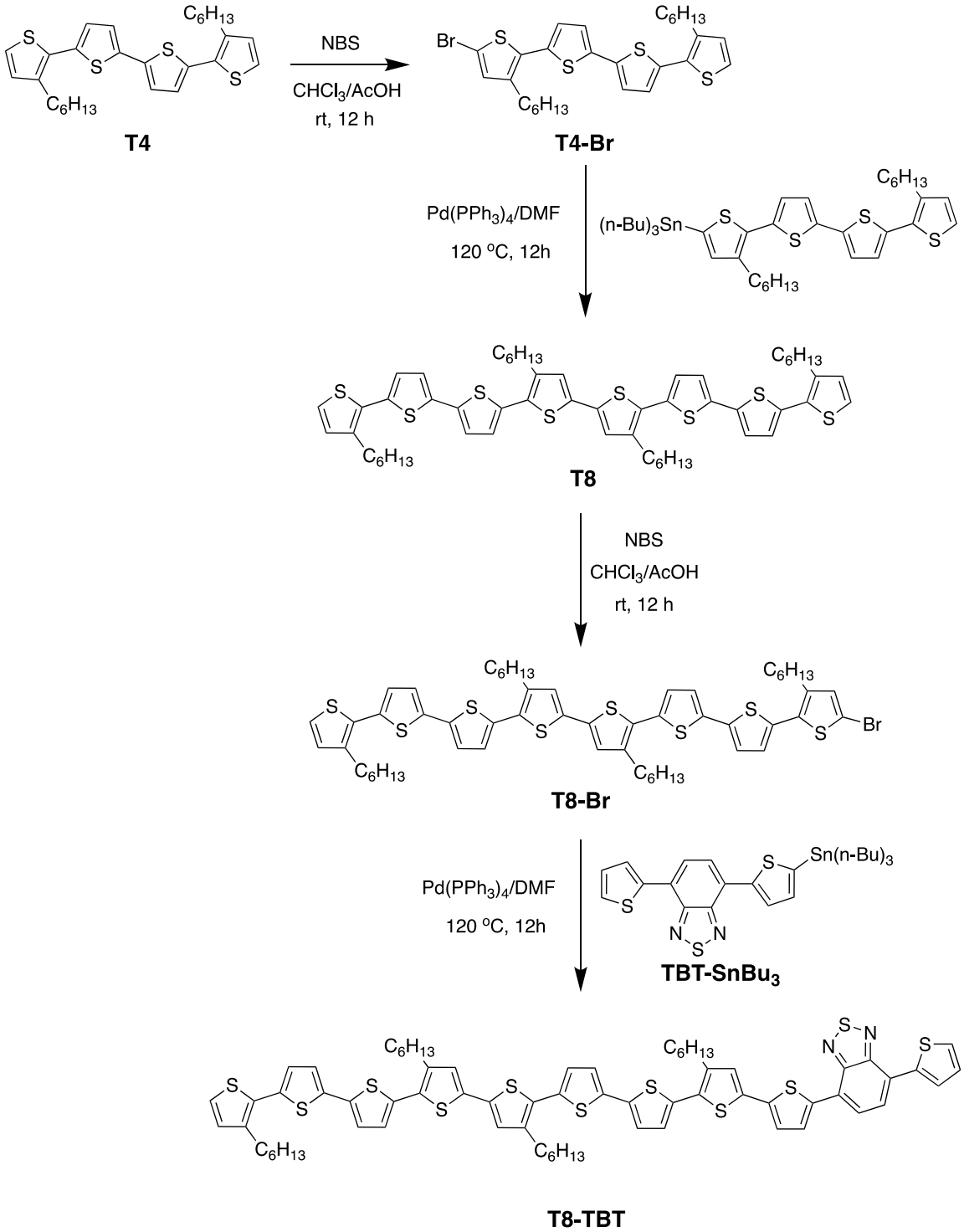


**Scheme S2.** Synthesis of **T8-TBT**.

**Synthesis of T4-TBT**: To a solution of **TBT-Br** (220 mg, 0.316 mmol) and **T4-SnBu$_3$** (274 mg, 0.348 mmol) DMF (20 mL) was added $Pd(PPh_3)_4$ (38 mg, 0.032 mmol). The reaction mixture was stirred at 120 $^oC$ for 12 h and the solvent was evaporated under reduced pressure. The crude product was purified by silica gel column chromatography using hexane/$CH_2Cl_2$ as eluent resulting in a wine red color solid (227 mg, 90%).

$^1H$ NMR (500 MHz, $CDCl_3$): δ (ppm) 8.13 (dd, 1H), 8.04 (d, 1H), 7.88 (quartet, 2H), 7.47 (dd, 1H), 7.25 (d, 1H), 7.27 – 7.13 (m, 5H), 7.08 (d, 1H), 7.04 (d, 1H), 6.95 (d, 1H), 2.78 – 2.74 (m, 8H), 1.75 – 1.60 (m, 8H), 1.40 -1.32 (m, 24H), 0.94 – 0.90 (m, 12H); $^{13}C$ NMR (125 MHz, $CDCl_3$): δ (ppm) 152.63, 152.45, 140.65, 139.90, 139.38, 138.57, 138.04, 136.92, 136.65, 135.47, 134.94, 134. 88, 130.30, 130.11, 129.97, 128.25, 128.04, 127.53, 127.02, 126.84, 126.54, 126.42, 125.89, 125.77, 125.58, 125.14, 124.41, 123.92, 123.89, 31.69, 30.65, 30.47, 29.60, 29.31, 29.24, 27.86, 26.86, 22.65, 17.54, 13.63. ESI-MS (m/z) $[M]^+$ Calculated for $C_{42}H_{40}N_2S_7$ : 796.1230 found: 796.1350.

**Synthesis of T8-TBT**: To a solution of **T8-Br** (75 mg, 0.070 mmol) and **TBT-SnBu$_3$** (45 mg, 0.077 mmol) DMF (10 mL) was added $Pd(PPh_3)_4$ (8 mg, 0.007 mmol). The reaction mixture was stirred at 120 $^oC$ for 12 h and the solvent was evaporated under reduced pressure. The crude product was purified by silica gel column chromatography using hexane/$CH_2Cl_2$ as eluent resulting in a brown color solid (77 mg, 85%).

$^1H$ NMR (500 MHz, $CDCl_3$): δ (ppm) 8.08 (dd, 1H), 7.95 (d, 1H), 7.78 (quartet, 2H) 7.43 (d, 1H), 7.26 – 7.09 (m, 8H), 7.02 – 6.94 (m, 7H), 2.78 – 2.74 (m, 8H), 1.75 – 1.60 (m, 8H), 1.40 -1.32 (m, 24H), 0.94 – 0.90 (m, 12H); $^{13}C$ NMR (125 MHz, $CDCl_3$): δ (ppm) 152.57, 152.38, 140.48, 139.86, 139.38, 138.53, 137.98, 136.70, 135.41, 134.98, 134.80, 130.34, 130.11129.99, 129.55, 128.19, 128.00, 127.47, 126.94, 126.76, 126.57, 126.49, 126.25, 126.18, 125.76, 125.68, 125.49, 125.01, 124.35, 123.91, 123.85, 31.73, 31.71, 30.65, 30.42, 29.74, 29.68, 29.62, 29.37, 29.33, 29.26, 22.67, 14.17, 14.14. ESI-MS (m/z) $[M]^+$ Calculated for $C_{70}H_{72}N_2S_{11}$: 1292.2612, found: 1292.2618.

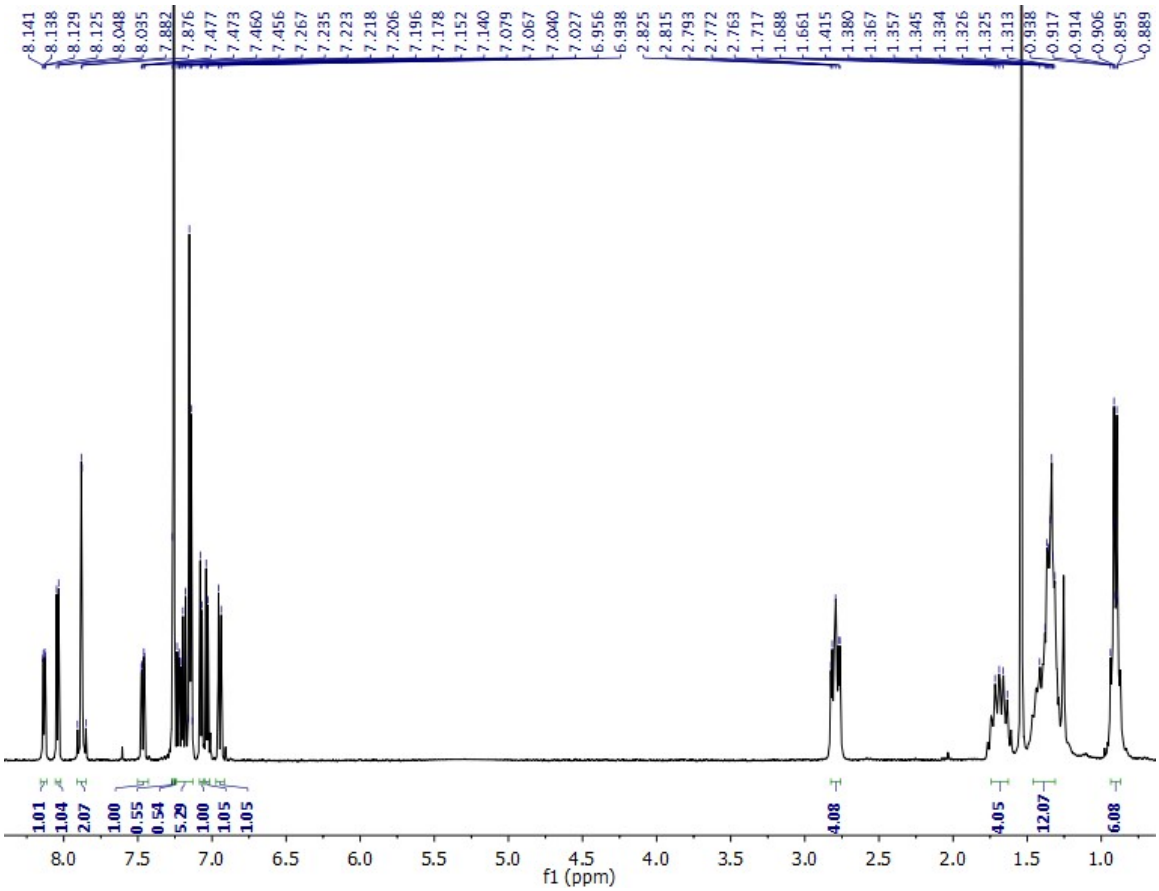


**Figure S1.** $^{1}$H NMR spectrum (500 MHz, $CDCl_3$) of **T4-TBT**.

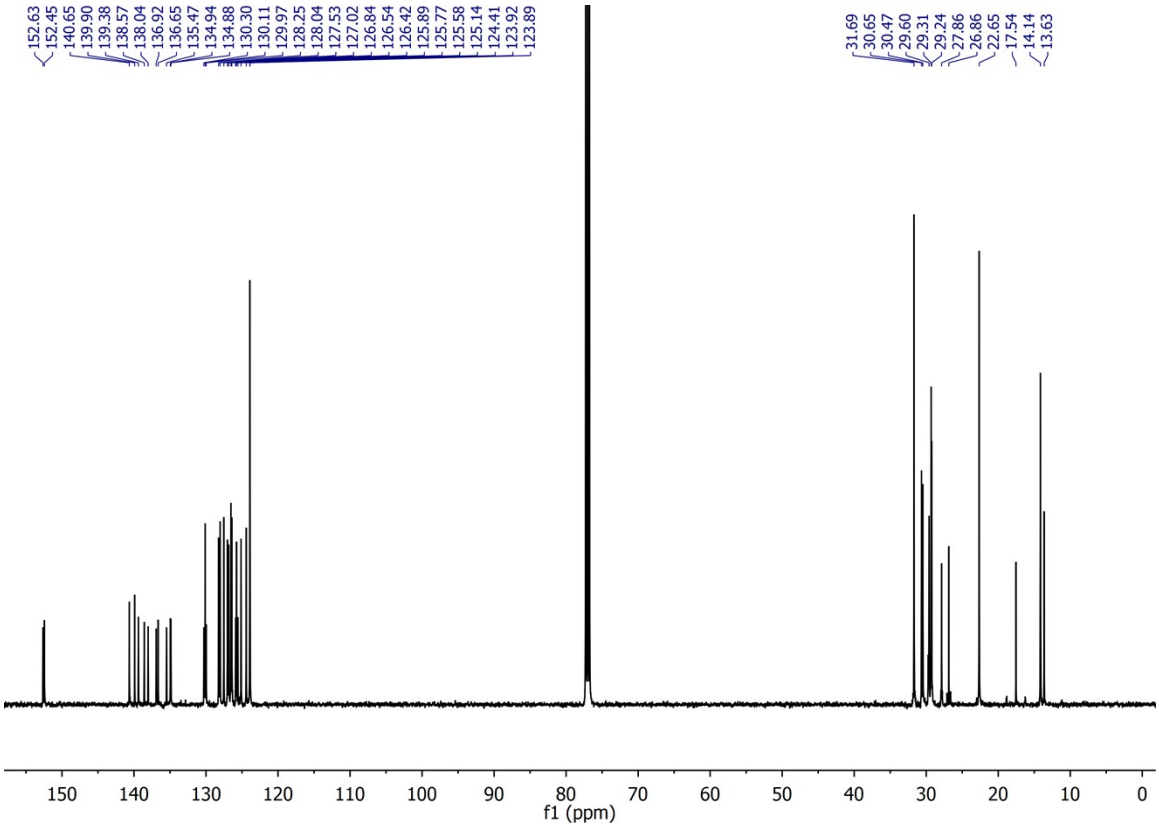


**Figure S2.** $^{13}C$ NMR spectrum (125 MHz, $CDCl_3$) of **T4-TBT**.

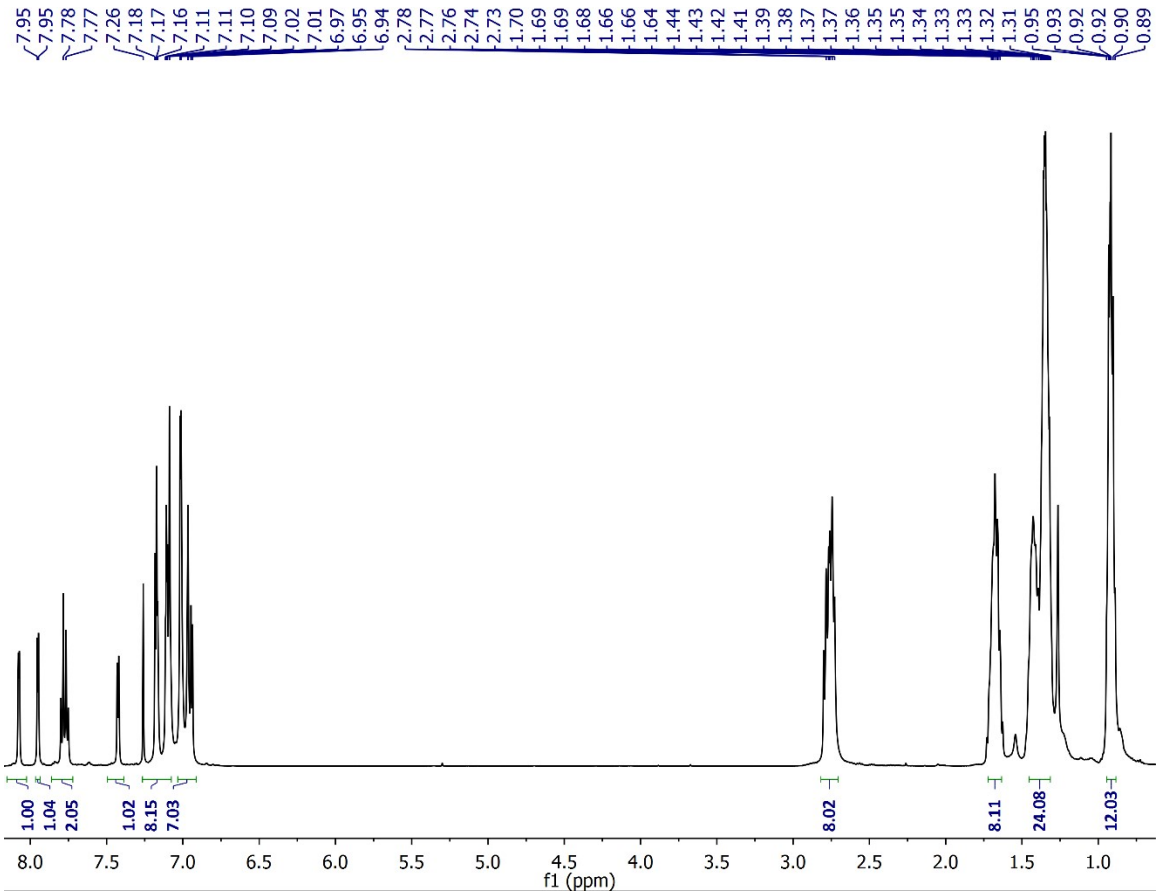


**Figure S3.** $^{1}$H NMR spectrum (500 MHz, $CDCl_3$) of **T8-TBT**.

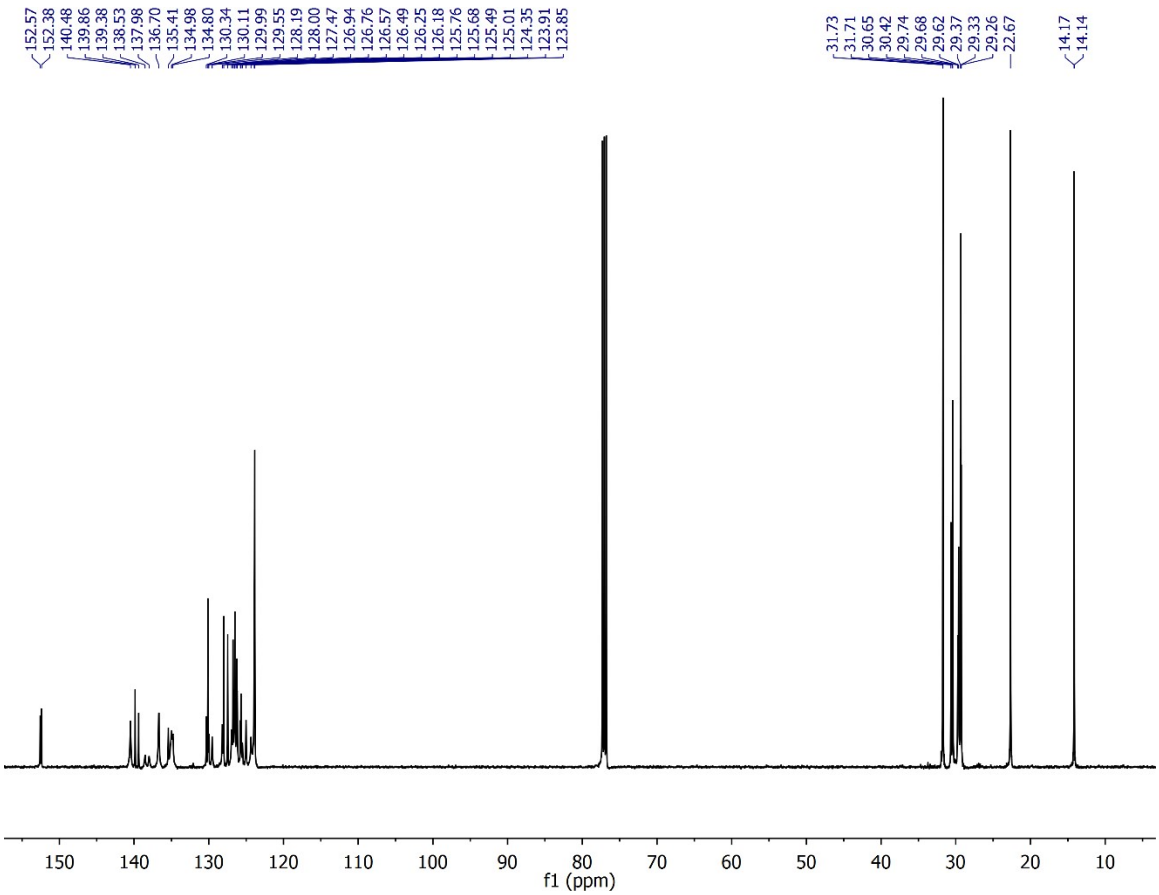


**Figure S4.** $^{13}C$ NMR spectrum (125 MHz, $CDCl_3$) of **T8-TBT**.

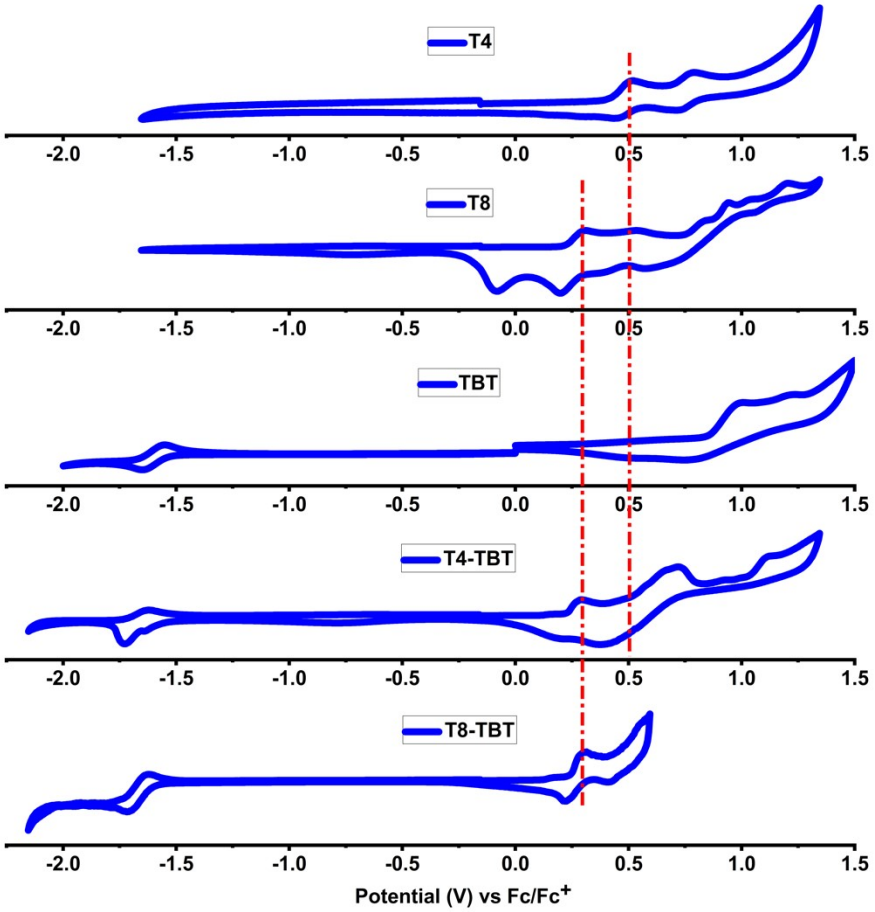


**Figure S5**. Cyclic voltammograms of **T4**, **T8**, **TBT**, **T4-TBT**, and **T8-TBT** in nitrogen saturated dichloromethane with 0.1 M tetrabutyl ammonium hexafluoro phosphate as a supporting electrolyte in a three-electrode set up with glassy carbon (WE), silver/silver chloride (RE), and platinum wire (CE) and a scan rate of 100 $mVs^{-1}$

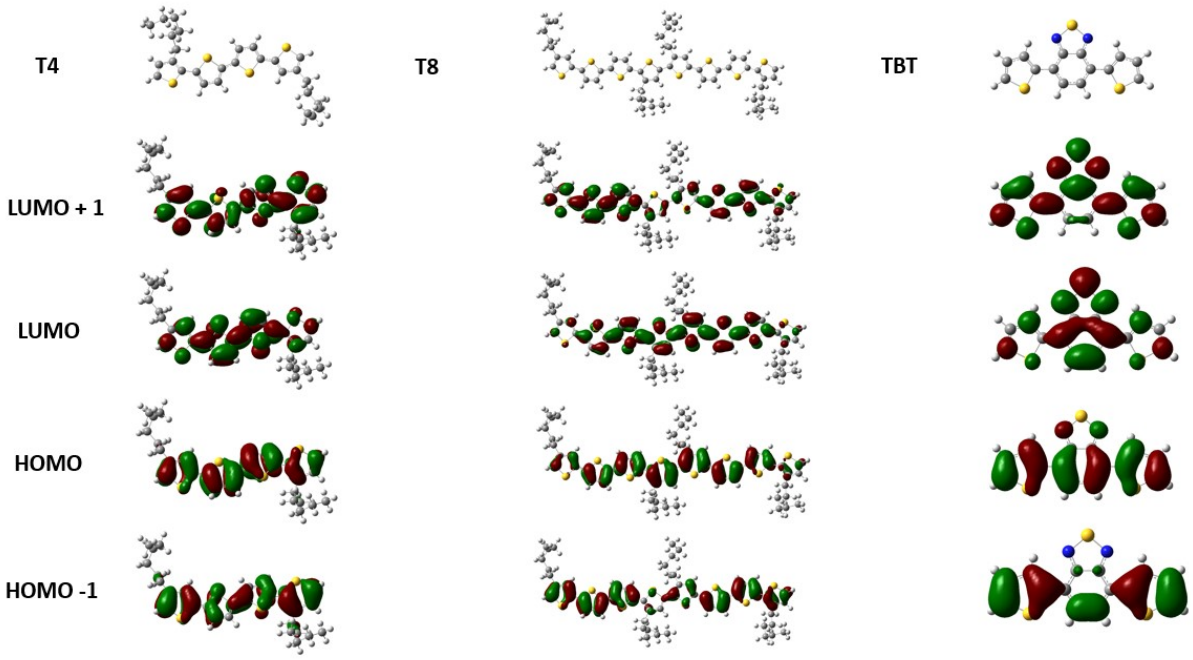


**Figure S6**. HOMO-LUMO frontier orbitals of model compounds **T4**, **T8**, and **TBT.**

**Table S1**. **Frontier Energy Level Energies for T4, T8 and TBT**[a]

| Compound | LUMO +1 | LUMO | HOMO | HOMO -1 |
|---|---|---|---|---|
| **T4** | - 0.78 | - 1.74 | - 4.98 | - 5.97 |
| **T8** | - 1.69 | - 2.05 | - 4.75 | - 5.15 |
| **TBT** | - 1.08 | - 2.61 | - 5.35 | - 6.59 |

[a] Energies listed in eV relative to vacuum level.

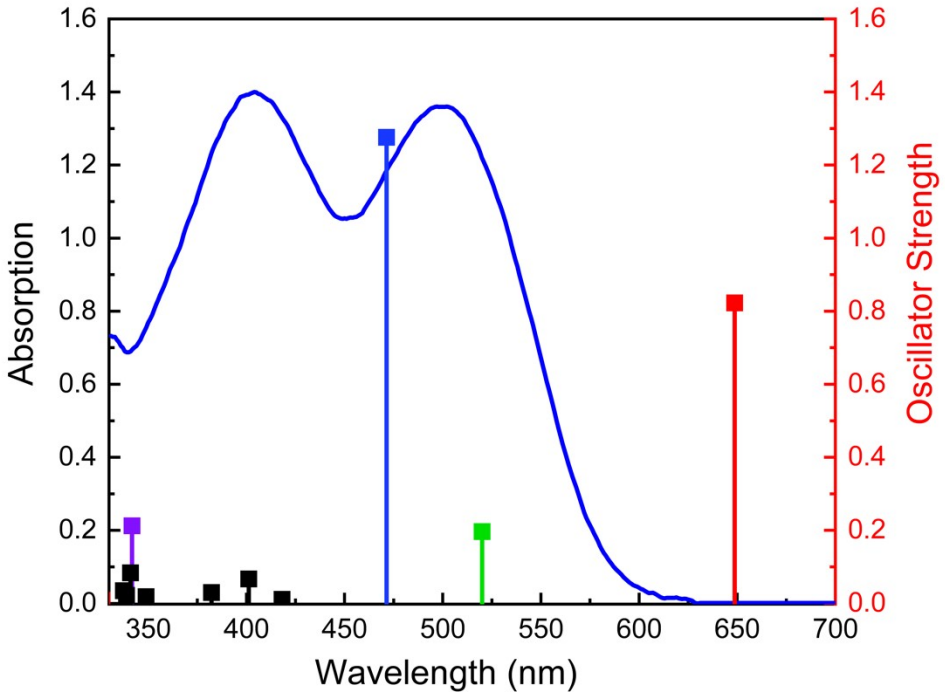


**Figure S7**. Experimentally measured UV-vis spectra (blue) in hexane and TDDFT calculated transitions (symbol and lines) for **T4-TBT**

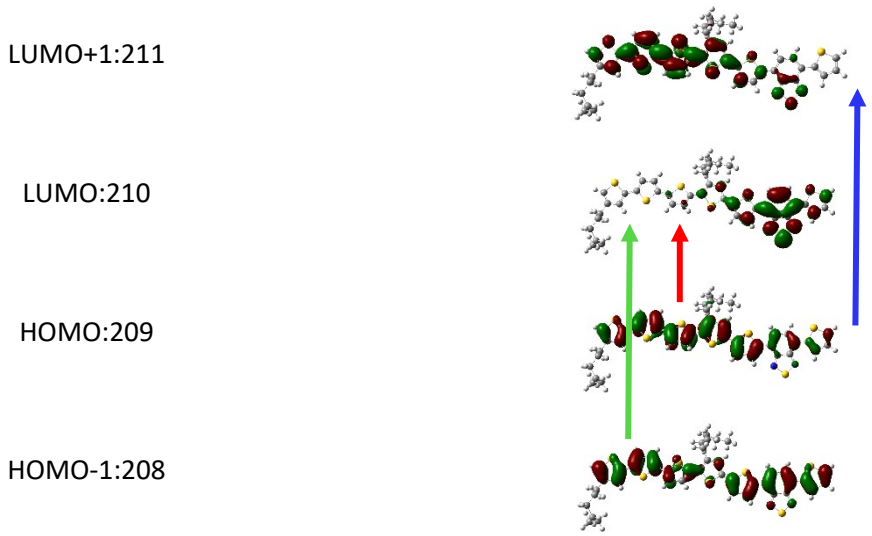


**Figure S8**. Frontier molecular orbitals (HOMO and LUMO) of **T4-TBT**. Lines show major transitions with oscillator strength higher than 0.15.

**Table S2**. Table of transitions for **T4-TBT**. Major transitions with oscillator strength higher than **0.15** are shown in color (bold)

| Excited State | Excitation transitions | | Energy (eV) | Wavelength (nm) | Oscillator strength (f) |
|---|---|---|---|---|---|
| 1 | 209 ->210 | 0.69962 | 1.9113 | **648.69** | **0.8224** |
| 2 | 208 ->210 | 0.68703 | 2.3840 | **520.07** | **0.1964** |
| 3 | 209 ->211 | 0.68882 | 2.6301 | **471.41** | **1.2760** |
| 4 | 207 ->210 | 0.67716 | 2.9651 | 418.14 | 0.0110 |
| 5 | 208 ->211 | 0.53864 | 3.0902 | 401.22 | 0.0670 |
| | 209 ->212 | -0.44195 | | | |
| 6 | 208 ->211 | 0.42573 | 3.2436 | 382.24 | 0.0299 |
| | 209 ->212 | 0.51751 | | | |
| 7 | 205 ->210 | 0.16898 | 3.5536 | 348.89 | 0.0186 |
| | 206 ->210 | 0.62436 | | | |
| | 208 ->212 | -0.17512 | | | |
| 8 | 201 ->210 | -0.20796 | 3.6284 | **341.70** | **0.2125** |
| | 203 ->210 | 0.12114 | | | |
| | 204 ->210 | -0.35558 | | | |
| | 206 ->210 | 0.11802 | | | |
| | 207 ->211 | 0.22771 | | | |
| | 208 ->212 | 0.39323 | | | |
| | 209 ->213 | 0.26845 | | | |
| 9 | 201 ->210 | 0.13220 | 3.6360 | 340.99 | 0.0836 |
| | 203 ->210 | 0.21422 | | | |
| | 204 ->210 | 0.27850 | | | |
| | 206 ->210 | 0.13208 | | | |
| | 207 ->211 | -0.11090 | | | |
| | 208 ->212 | 0.46654 | | | |
| | 209 ->213 | -0.28403 | | | |
| | 209 ->214 | 0.10833 | | | |
| 10 | 203 ->210 | 0.59834 | 3.6576 | 338.97 | 0.0220 |
| | 204 ->210 | 0.18031 | | | |
| | 207 ->211 | 0.10375 | | | |
| | 208 ->212 | -0.22041 | | | |
| | 209 ->213 | 0.19703 | | | |
| 11 | 201 ->210 | 0.16371 | 3.6752 | 337.36 | 0.0348 |
| | 203 ->210 | -0.25127 | | | |
| | 204 ->210 | 0.40621 | | | |
| | 207 ->211 | 0.36223 | | | |
| | 208 ->212 | 0.10076 | | | |

| | | | | | |
|---|---|---|---|---|---|
| | 209 ->213 | 0.28854 | | | |
| 12 | 201 ->210 | 0.51064 | 3.7975 | 326.49 | 0.0086 |
| | 204 ->210 | -0.25974 | | | |
| | 205 ->210 | -0.24937 | | | |
| | 206 ->210 | 0.15018 | | | |
| | 207 ->211 | 0.19053 | | | |
| | 209 ->213 | -0.11304 | | | |
| | 209 ->214 | -0.11754 | | | |
| 13 | 205 ->210 | 0.43407 | 3.8236 | 324.26 | 0.0397 |
| | 206 ->210 | -0.10209 | | | |
| | 207 ->211 | 0.37663 | | | |
| | 209 ->213 | -0.34250 | | | |
| 14 | 201 ->210 | 0.33427 | 3.8397 | 322.90 | 0.0255 |
| | 204 ->210 | -0.12982 | | | |
| | 205 ->210 | 0.45071 | | | |
| | 207 ->211 | -0.25899 | | | |
| | 209 ->213 | 0.25297 | | | |
| 15 | 202 ->210 | -0.19890 | 3.9550 | 313.49 | 0.0060 |
| | 206 ->211 | 0.17124 | | | |
| | 207 ->211 | 0.15866 | | | |
| | 207 ->212 | 0.10461 | | | |
| | 209 ->214 | 0.57737 | | | |
| 16 | 200 ->210 | -0.12130 | 4.0106 | 309.14 | 0.0032 |
| | 202 ->210 | 0.64941 | | | |
| | 209 ->214 | 0.18323 | | | |
| 17 | 198 ->210 | -0.10263 | 4.1144 | 301.34 | 0.0110 |
| | 199 ->210 | 0.46428 | | | |
| | 200 ->210 | 0.44102 | | | |
| | 209 ->215 | -0.15507 | | | |
| 18 | 198 ->210 | 0.25231 | 4.1560 | 298.32 | 0.0567 |
| | 207 ->212 | 0.10836 | | | |
| | 208 ->213 | 0.59735 | | | |
| | 209 ->214 | -0.10643 | | | |
| 19 | 198 ->210 | 0.25025 | 4.1944 | 295.59 | 0.0145 |
| | 199 ->210 | -0.26868 | | | |
| | 200 ->210 | 0.45642 | | | |
| | 202 ->210 | 0.11935 | | | |
| | 206 ->211 | -0.12095 | | | |
| | 208 ->213 | -0.15217 | | | |
| | 208 ->214 | 0.13704 | | | |
| | 209 ->215 | 0.21220 | | | |

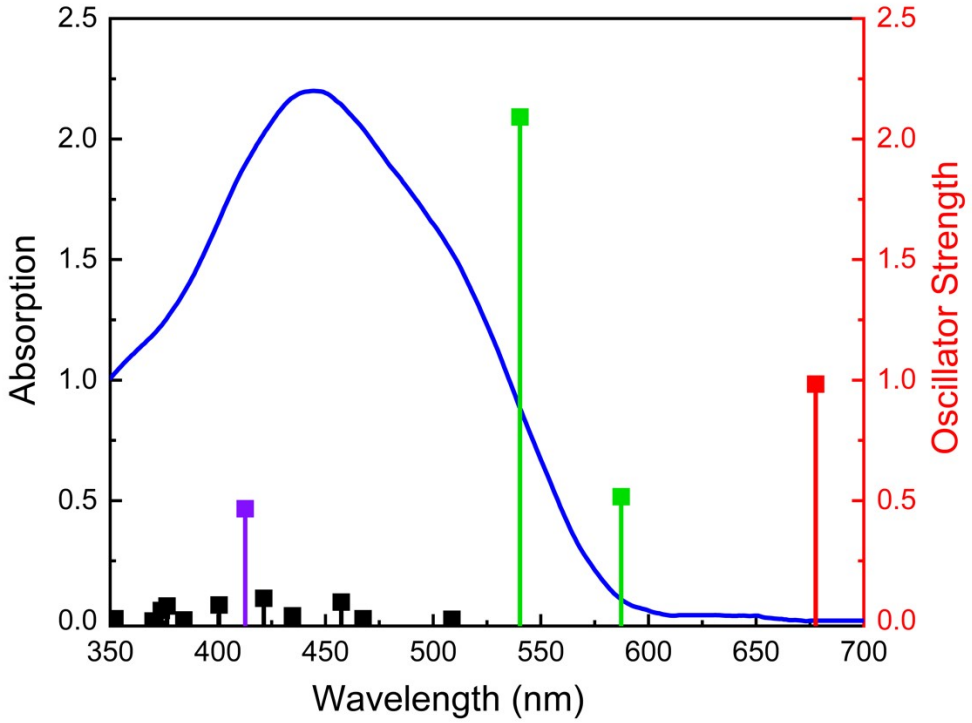


**Figure S9**. Experimentally measured UV-vis spectra (blue) in hexane and TDDFT calculated transitions (symbol and lines) for **T8-TBT**

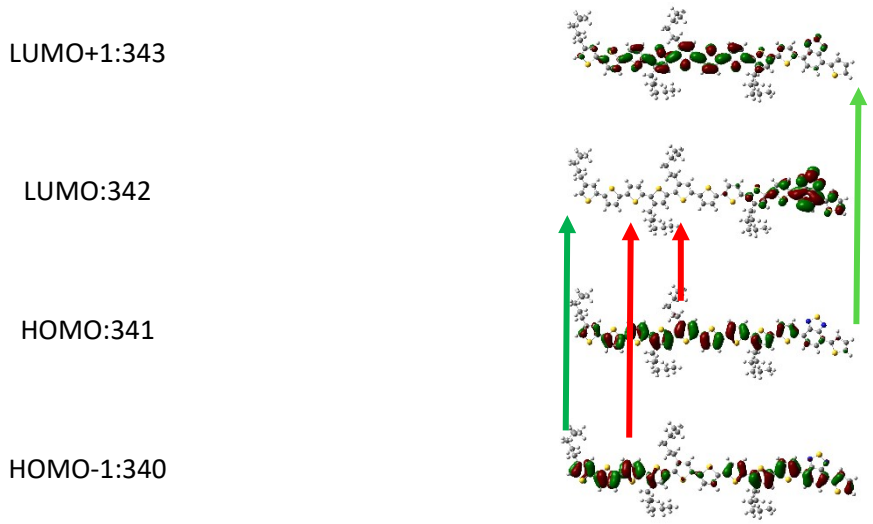


**Figure S10**. Frontier molecular orbitals (HOMO and LUMO) of **T8-TBT**. Lines show major transitions with oscillator strength higher than 0.15.

**Table S3**. Table of transitions for **T8-TBT**. Major transitions with oscillator strength higher than **0.15** are shown in color (bold)

| Excited State | Excitation transitions | | Energy (eV) | Wavelength (nm) | Oscillator strength (f) |
|---|---|---|---|---|---|
| 1 | 340 -> 342 | 0.69962 | 1.8296 | **677.66** | **0.9836** |
| | 341 -> 342 | 0.67518 | | | |
| 2 | 339 -> 342 | 0.14381 | 2.1110 | **587.34** | **0.5162** |
| | 340 -> 342 | 0.64742 | | | |
| | 341 -> 342 | 0.20012 | | | |
| | 341 -> 343 | 0.11942 | | | |
| 3 | 340 -> 342 | -0.14960 | 2.2945 | **540.35** | **2.0912** |
| | 340 -> 344 | -0.13127 | | | |
| | 341 -> 343 | 0.67189 | | | |
| 4 | 338 -> 342 | 0.10139 | 2.4371 | 508.73 | 0.0075 |
| | 339 -> 342 | 0.67323 | | | |
| | 340 -> 342 | -0.13852 | | | |
| 5 | 340 -> 343 | 0.64878 | 2.6522 | 467.47 | 0.0102 |
| | 341 -> 344 | 0.24058 | | | |
| 6 | 340 -> 343 | -0.23617 | 2.7111 | 457.33 | 0.0789 |
| | 340 -> 345 | 0.10084 | | | |
| | 341 -> 344 | 0.64157 | | | |
| 7 | 337 -> 342 | -0.16022 | 2.8522 | 434.70 | 0.0219 |
| | 338 -> 342 | 0.65645 | | | |
| 8 | 339 -> 343 | 0.54227 | 2.9424 | 421.38 | 0.0951 |
| | 340 -> 344 | -0.11149 | | | |
| | 341 -> 345 | -0.41153 | | | |
| 9 | 340 -> 344 | 0.64026 | 3.0039 | **412.74** | **0.4660** |
| | 341 -> 343 | 0.13306 | | | |
| | 341 -> 345 | -0.22897 | | | |
| 10 | 337 -> 342 | 0.11404 | 3.0951 | 400.58 | 0.0670 |
| | 339 -> 343 | 0.42185 | | | |
| | 340 -> 344 | 0.16897 | | | |
| | 341 -> 345 | 0.48413 | | | |
| 11 | 336 -> 342 | 0.14925 | 3.2265 | 384.26 | 0.0047 |
| | 337 -> 342 | 0.60676 | | | |
| | 338 -> 342 | 0.14398 | | | |
| | 340 -> 345 | -0.17974 | | | |
| | 341 -> 345 | -0.12047 | | | |
| 12 | 337 -> 342 | 0.12671 | 3.2935 | 376.45 | 0.0626 |
| | 338 -> 343 | 0.17440 | | | |
| | 339 -> 344 | 0.45766 | | | |
| | 340 -> 345 | 0.38260 | | | |
| | 341 -> 346 | 0.25371 | | | |
| 13 | 337 -> 342 | 0.16244 | 3.3167 | 373.82 | 0.0443 |
| | 338 -> 343 | 0.10176 | | | |

| | | | | | |
|---|---|---|---|---|---|
| | 339 -> 344 | -0.41696 | | | |
| | 340 -> 345 | 0.48181 | | | |
| | 341 -> 346 | -0.13022 | | | |
| 14 | 338 -> 343 | 0.43978 | 3.3517 | 369.91 | 0.0004 |
| | 339 -> 344 | -0.24155 | | | |
| | 340 -> 345 | -0.19630 | | | |
| | 341 -> 346 | 0.40963 | | | |
| 15 | 338 -> 343 | 0.48312 | 3.5202 | 352.20 | 0.0098 |
| | 339 -> 344 | 0.13500 | | | |
| | 341 -> 346 | -0.44511 | | | |
| 16 | 331 -> 342 | -0.15926 | 3.6078 | **343.65** | **0.2050** |
| | 336 -> 342 | -0.23509 | | | |
| | 339 -> 345 | 0.59043 | | | |
| 17 | 333 -> 342 | -0.27994 | 3.6240 | 342.12 | 0.0134 |
| | 336 -> 342 | 0.11734 | | | |
| | 337 -> 343 | 0.18974 | | | |
| | 338 -> 344 | -0.22888 | | | |
| | 339 -> 345 | 0.12136 | | | |
| | 340 -> 346 | 0.33262 | | | |
| | 341 -> 347 | 0.34634 | | | |
| | 341 -> 348 | -0.14380 | | | |
| 18 | 328 -> 342 | 0.11151 | 3.6438 | 340.26 | 0.0655 |
| | 329 -> 342 | 0.16449 | | | |
| | 331 -> 342 | 0.25215 | | | |
| | 333 -> 342 | 0.26880 | | | |
| | 335 -> 342 | -0.12203 | | | |
| | 336 -> 342 | 0.42957 | | | |
| | 337 -> 342 | -0.13089 | | | |
| | 339 -> 345 | 0.27631 | | | |
| 19 | 329 -> 342 | -0.10587 | 3.6566 | 339.07 | 0.0005 |
| | 331 -> 342 | 0.58004 | | | |
| | 333 -> 342 | 0.13549 | | | |
| | 336 -> 342 | -0.28905 | | | |
| 20 | 328 -> 342 | 0.10166 | 3.6710 | 337.74 | 0.0226 |
| | 329 -> 342 | 0.13190 | | | |
| | 331 -> 342 | -0.21817 | | | |
| | 333 -> 342 | 0.47234 | | | |
| | 336 -> 342 | -0.12709 | | | |
| | 337 -> 343 | 0.16745 | | | |
| | 338 -> 344 | -0.17854 | | | |
| | 339 -> 345 | -0.12149 | | | |
| | 341 -> 346 | -0.10122 | | | |
| | 341 -> 347 | 0.23560 | | | |

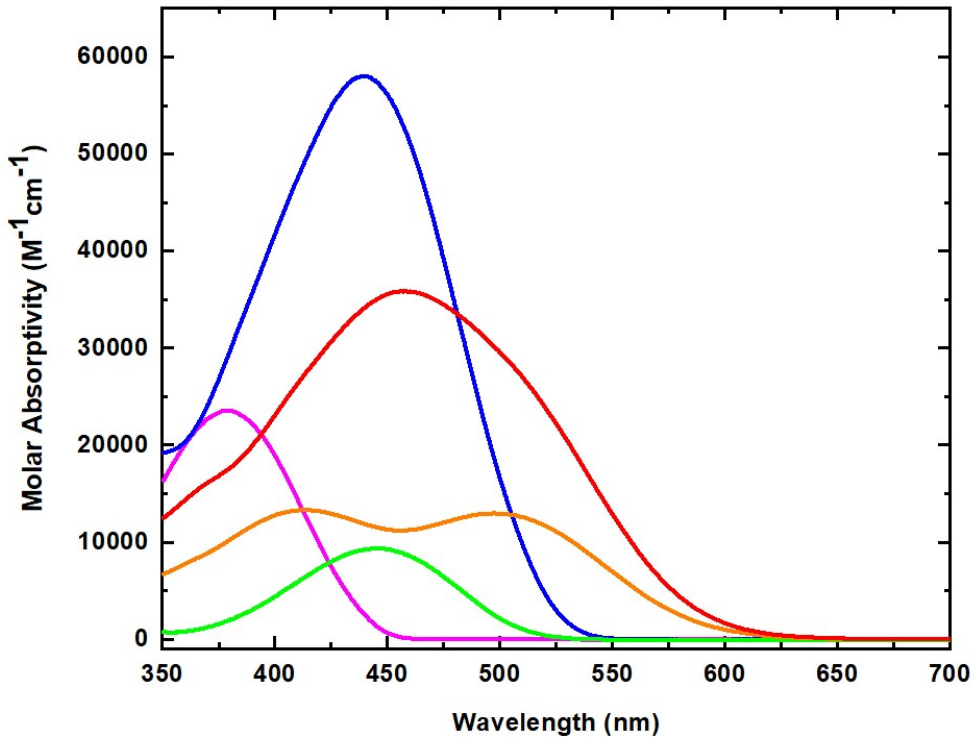


**Figure S11**. Uv-vis absorption spectra as a function of molar extinction coefficient measured in dichloromethane of **T4** (magenta), **T8** (blue), **TBT** (green), **T4-TBT** (orange), and **T8-TBT** (red).

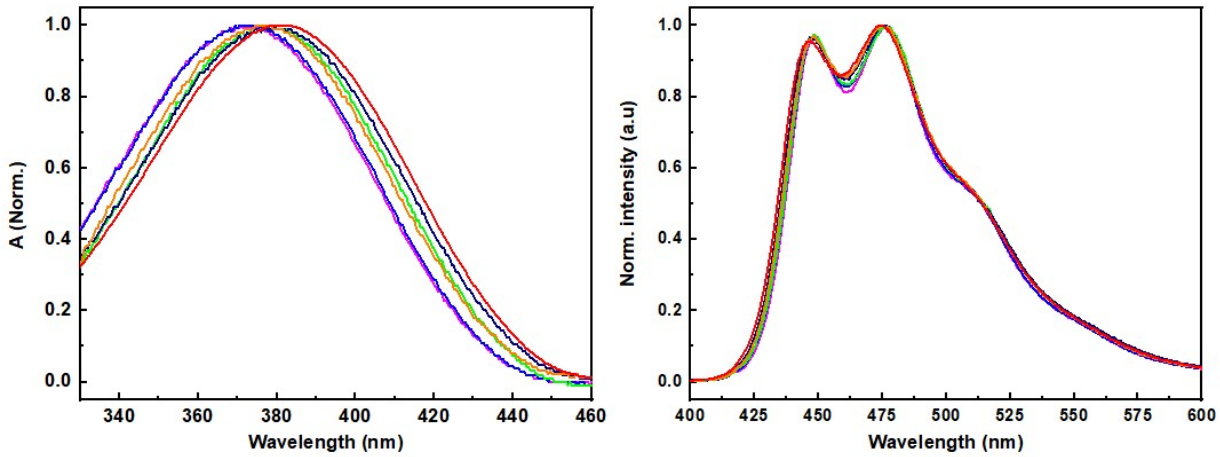


**Figure S12**. UV-vis absorption Spectra (left) and fluorescence emission (right) of **T4** in hexane (magenta), diethyl ether (blue), tetrahydrofuran (green), dichloromethane (navy), acetone (orange), and dimethyl formamide (red).

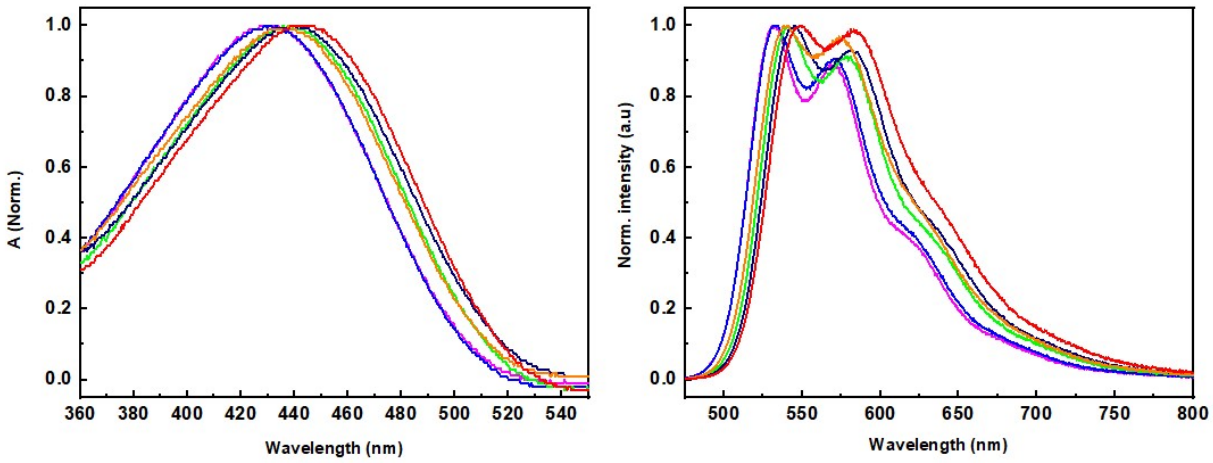


**Figure S13**. UV-vis absorption Spectra (left) and fluorescence emission (right) of **T8** in hexane (magenta), diethyl ether (blue), tetrahydrofuran (green), dichloromethane (navy), acetone (orange), and dimethyl formamide (red).

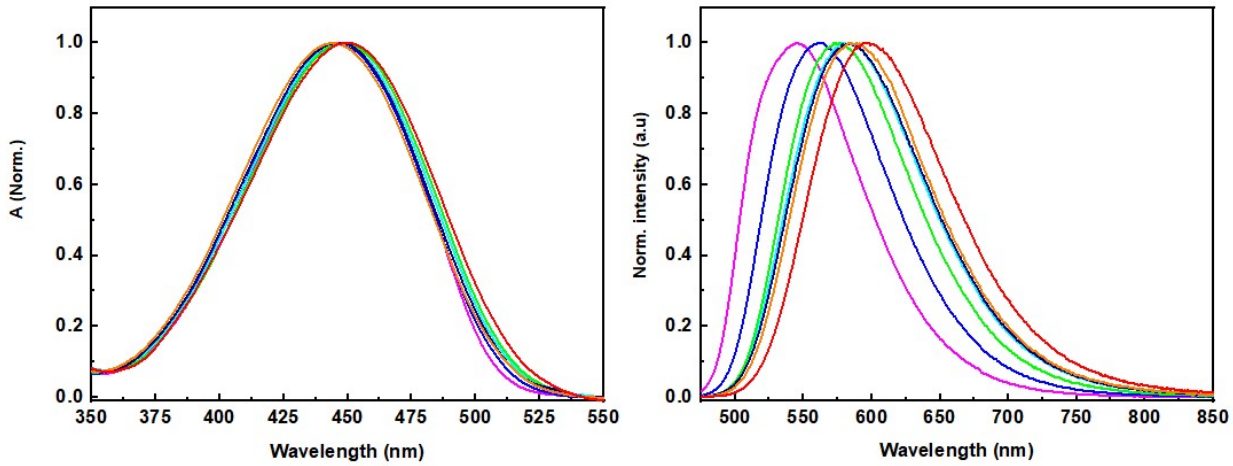


**Figure S14**. UV-vis absorption spectra (left) and fluorescence emission (right) of **TBT** in hexane (magenta), diethyl ether (blue), chloroform (cyan), tetrahydrofuran (green), dichloromethane (navy), acetone (orange), and dimethyl formamide (red).

**Lippert-Mataga Plots**

The Lippert-Mataga equation correlates the observed Stokes shift $(\Delta\nu)$ with the orientational polarizability of each of the molecules in the solvent medium, where $\nu_a$ and $\nu_e$ are the absorption and fluorescence maxima energies, respectively, $h$ is the Planck constant, $c$ is the light speed, $r$ is the molecular Onsager radius, $\Delta\mu$ is the dipole moment difference between the ground and excited states. The term $\frac{2\,(\Delta\mu)_2}{hc\ \ r^3}$ is the slope of the plot of $f(\varepsilon, n)$ vs $\Delta\nu$, and $\Delta\mu$ is obtained from the slope using the molecular Onsager radius and the physical constants $h$ and $c$.

$$\Delta\nu = \nu_a - \nu_e = \frac{2\,(\Delta\mu)_2}{hc\ \ r^3} f(\varepsilon, n) + C \tag{S1}$$

$$f(\varepsilon, n) = \left(\frac{\varepsilon - 1}{2\varepsilon + 1} - \frac{n^2 - 1}{2n^2 + 1}\right) \tag{S2}$$

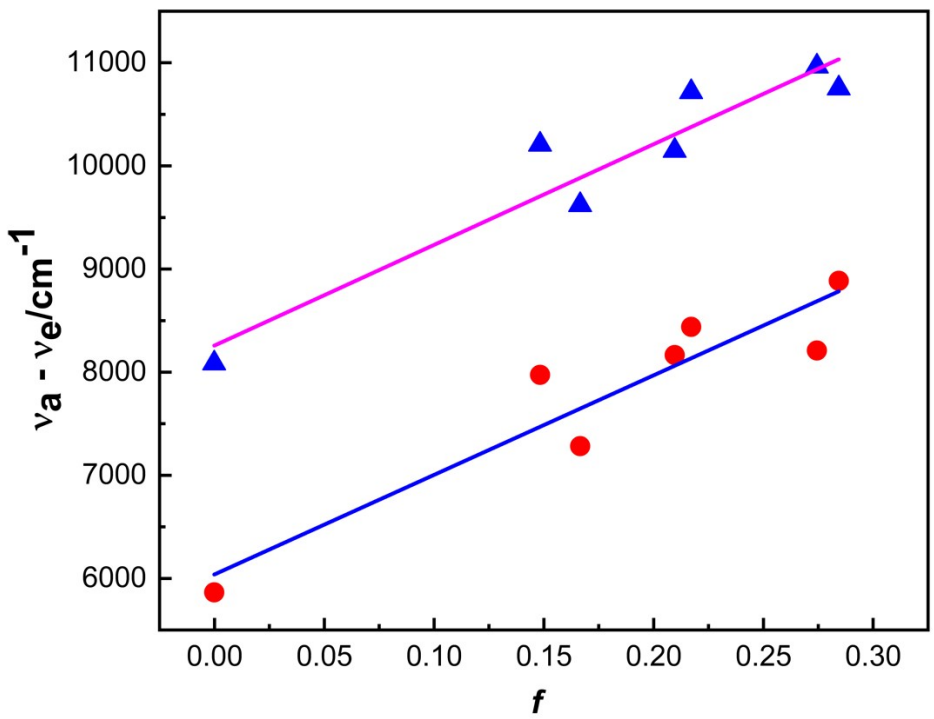


**Figure S15**. Lippert-Mataga plots of fluorescence data for **T4-TBT** and **T8-TBT** according to eqs. S1 and S2. (□) : **T4-TBT**. (●): **T8-TBT**. Solid lines are least squares fits of the data.

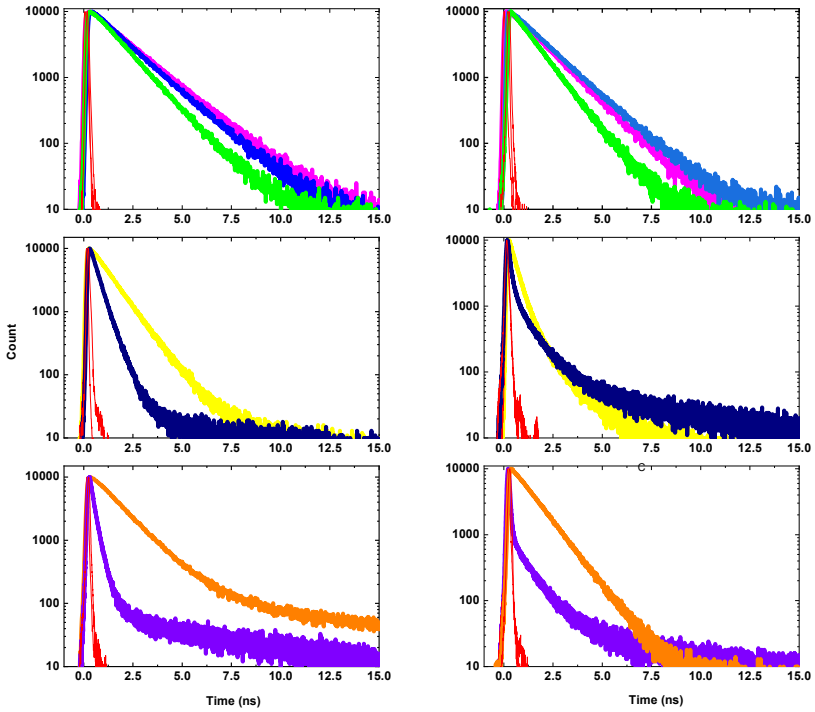


**Figure S16**. Fluorescence emission decays of **T4-TBT** (left column) and **T8-TBT** (right column) in different solvents: hexane (magenta), diethyl ether (blue), chloroform (green), dichloromethane (yellow), acetone (navy), tetrahydrofuran (orange), and dimethyl formamide (violet)

**Table S4. Rates of radiative and non-radiative processes [a]**

| | T4-TBT | | | T8-TBT | | |
|---|---|---|---|---|---|---|
| **Solvent** | **τ / ns** | $k_r$ / $10^8$ $s^{-1}$ | $k_{nr}$ / $10^8$ $s^{-1}$ | **τ / ns** | $k_r$ / $10^8$ $s^{-1}$ | $k_{nr}$ / $10^8$ $s^{-1}$ |
| **Hex** | 1.8 | 1.9 | 3.4 | 1.5 | 2.6 | 4.1 |
| **Et2O** | 1.6 | 1.6 | 4.7 | 1.5 | 1.7 | 5.0 |
| **THF** | 1.63 | 1.1 | 5.0 | 1.1 | 1.3 | 7.8 |
| **CHCl3** | 1.3 | 1.2 | 6.5 | 1.1 | 1.3 | 7.8 |
| **DCM** | 1.3 | 0.77 | 6.9 | 0.55 | 0.54 | 17.6 |
| **Ace** | 0.42 | 0.71 | 23 | 0.52 | 0.20 | 19 |
| **DMF** | 0.23 | 3.9 | 39.6 | 0.23 | 0.09 | 43.4 |

[a] Calculated according to the expressions $k_{nr} = 1/\tau$ and $k_r = \phi_{em}/\tau$ and $k_{nr} = k_r(1/\phi_{em} - 1)$ (see Table 2 in text for data). Median fluorescence lifetimes used when decays were biexponential. Median lifetimes calculated by using the following equation: $\langle\tau\rangle = \Sigma\alpha_i\tau_i$ where $\alpha_i$ and $\tau_I$ are the normalized amplitude and lifetime for the decay components.

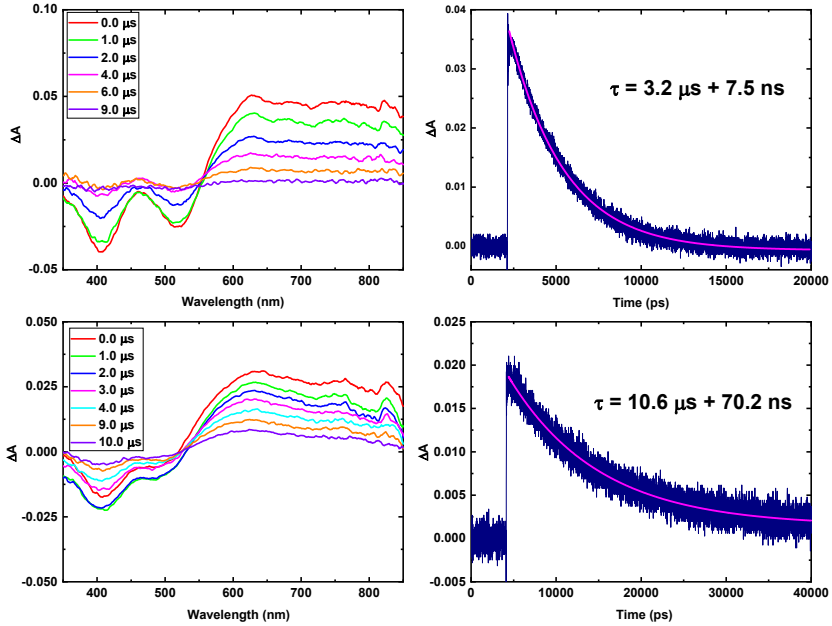


**Figure S17**. Nanosecond transient absorption of T4-TBT ($\lambda_{ex}$ = 410 nm, 4 mJ/pulse, 5 ns fwhm) in hexane (top) and dichloromethane (bottom) along with time profile kinetic fit at 630 nm for both hexane and dichloromethane.

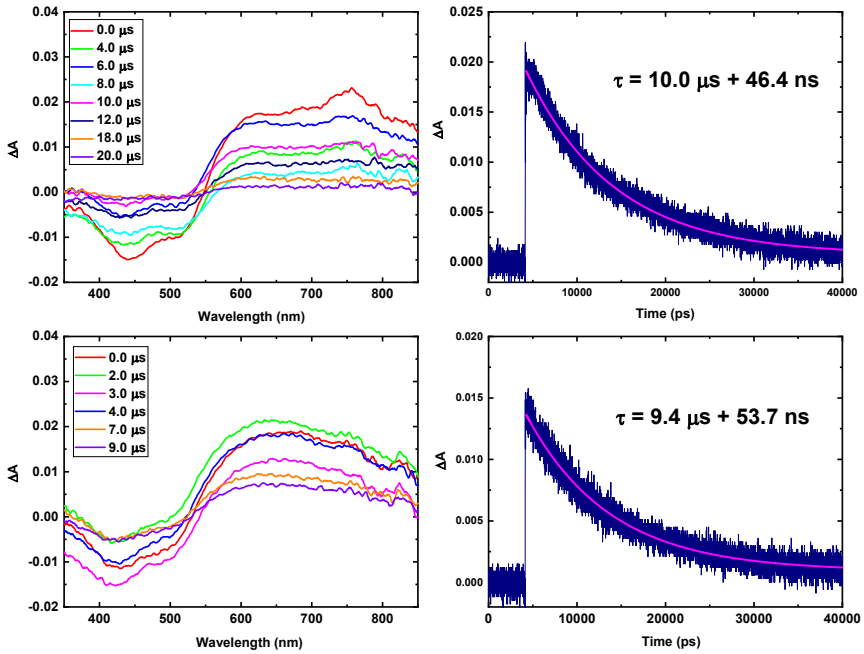


**Figure S18**. Nanosecond transient absorption of T8-TBT ($\lambda_{ex}$ = 410 nm, 4 mJ/pulse, 5 ns fwhm) in hexane (top) and dichloromethane (bottom) along with the decay profile at 615 nm and 640 nm.

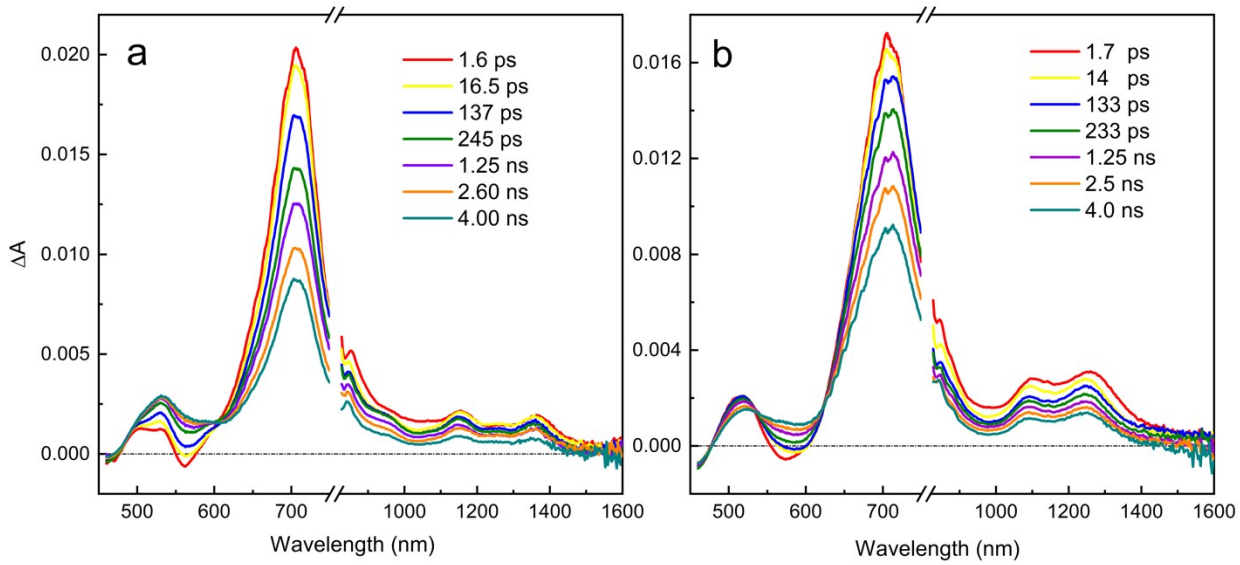


**Figure S19.** Femtosecond TA spectra of **TBT** in hexane (a) and in dichloromethane (b) at excitation wavelength of 450 nm.

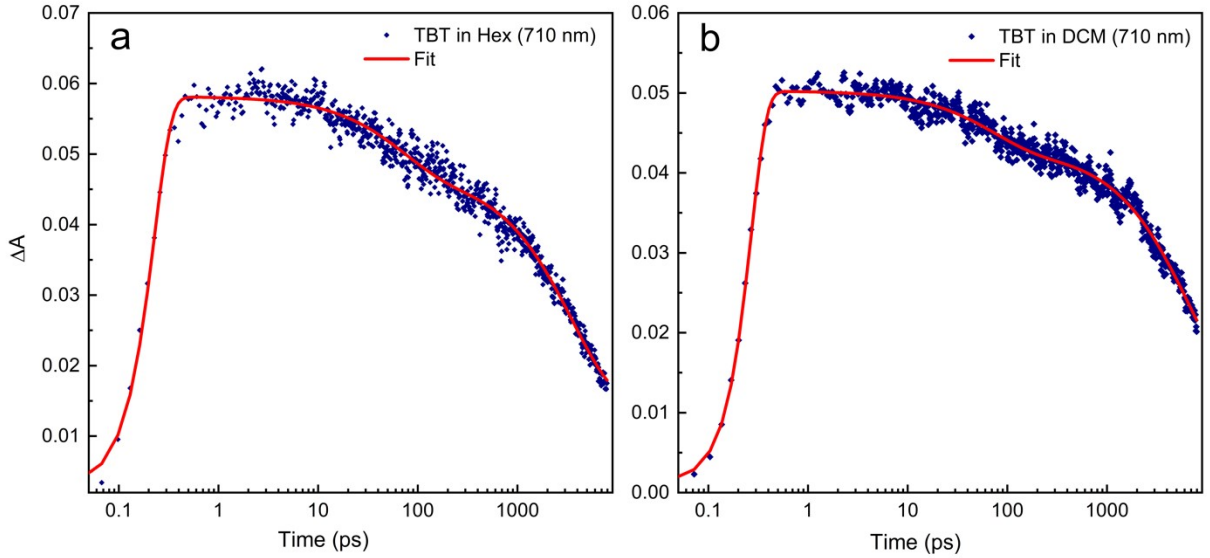


**Figure S20.** Decay traces at 710 nm with exponential fits for **TBT** in hexane (a) and dichloromethane (b)

**Table S5. Time constants for bi-exponential fit @ 710 nm for TBT transient absorption decays in hexane and dichloromethane**

| Solvent | TBT | | |
|---|---|---|---|
| | $\tau_1$ | $\tau_2$ | $A_{inf}$ |
| **Hexane** | 67.5 ps (5.8%) | 3.6 ns (56.2%) | 38% |
| **DCM** | 69.3 ps (14.8%) | 6.5 (59.7%) | 25.5% |

The energy of the charge transfer state is estimated calculated the Weller equation (eq. S-3).[8-10] In eq. S-1, $E_{1/2ox}$ is the first oxidation potential of $\mathbf{T_4}$ and $\mathbf{T_8}$ and $E_{1/2red}$ is the first reduction potential of **TBT**, r is the center-to-center distance of the (+) and (-) charges in the charge-separated state, e is the charge of an electron, $\varepsilon_0$ is the vacuum permittivity constant, $\varepsilon_s$ is the dielectric constant of of the solvent, $r^+$ and $r^-$ are the radii of the positive and negative ions, and $\varepsilon_{ref}$ is the reference solvent dielectric constant, DCM (8.93). The center-to-center distance and the radical ion radii are estimated from the DFT (B3LYP; 6-31/G (d, p)) optimized geometries.

$$E_{CT} = E_{1/2ox} - E_{1/2red} - e^2/4\pi\varepsilon_0\varepsilon_s r - e^2/8\pi\varepsilon_0(1/r^+ + 1/r^-)(1/\varepsilon_{ref} - 1/\varepsilon_s) \qquad \text{(S-3)}$$

**References for Supporting Information**


1. Stalder, R.; Xie, D.; Zhou, R.; Xue, J.; Reynolds, J. R.; Schanze, K. S. Variable-Gap Conjugated Oligomers Grafted to CdSe Nanocrystals. *Chem. Mater.* **2012**, *24*, 3143-3152.

2. Lu, C.; Fujitsuka, M.; Majima, T. Photoaccelerated Hole Transfer in Oligothiophene Assemblies. *J. Phys. Chem. C* **2017**, 1*21*, 649-655.

3. Cekli, S.; Winkel, R. W.; Schanze, K. S. Effect of Oligomer Length on Photophysical Properties of Platinum Acetylide Donor- Acceptor-Donor Oligomers. *J. Phys. Chem. A* **2016**, *120*, 5512-5521.

4. Jones, A. L.; Schanze, K. S. Fluorescent Charge-Transfer Excited States in Acceptor Derivatized Thiophene Oligomers. *J. Phys. Chem. A* **2020**, *124*, 7001-7013.

5. Gallaher, J. K.; Chen, K.; Huff, G. S.; Prasad, S. K. K.; Gordon, K. C.; Hodgkiss, J. M. Evolution of Nonmirror Image Fluorescence Spectra in Conjugated Polymers and Oligomers. *J. Phys. Chem. Lett.* **2016**, *7*, 3307-3312.

6. Kanato, H.; Narutaki, M.; Takimiya, K.; Otsubo, T.; Harima, Y. Synthesis and Photovoltaic Properties of Tetrathiafulvalene–Oligothiophene–Fullerene Triads. *Chem. Lett.* **2006**, *35*, 668-669.

7. Mulherin, R. C.; Jung, S.; Huettner, S.; Johnson, K.; Kohn, P.; Sommer, M.; Allard, S.; Scherf, U.; Greenham, N. C. Ternary Photovoltaic Blends Incorporating an All-Conjugated Donor-Accept- or Diblock Copolymer. *Nano Lett.* **2011**, *11*, 4846-4851.

8. Weller, A. Photoinduced Electron Transfer in Solution: Exciplex and Radical Ion Pair Formation Free Enthalpies and Their Solvent Dependence. **1982,** *133*, 93-98.

9. Kroon, J.; Oevering, H.; Verhoeven, J. W.; Warman, J. M.; Oliver, A. M.; Paddon-Row, M. N. Temperature Effects on Intramolecular Electron Transfer Kinetics under "Normal", "Inverted", and "Nearly Optimal" Conditions. *J. Phys. Chem.* **1993,** *97*, 5065-5069.

10. Oevering, H.; Paddon-Row, M. N.; Heppener, M.; Oliver, A. M.; Cotsaris, E.; Verhoeven, J. W.; Hush, N. S. Long-Range Photoinduced through-Bond Electron Transfer and Radiative Recombination Via Rigid Nonconjugated Bridges: Distance and Solvent Dependence. *J. Am. Chem. Soc.* **1987,** *109*, 3258-3269.